JOURNAL OF VIROLOGY, Nov. 2005, p. 13694–13704 Vol. 79, No. 21
0022-538X/05/$08.00+0 doi:10.1128/JVI.79.21.13694–13704.2005

Alternate Polypurine Tracts (PPTs) Affect the Rous Sarcoma Virus RNase H Cleavage Specificity and Reveal a Preferential Cleavage following a GA Dinucleotide Sequence at the PPT-U3 Junction

Kevin W. Chang,[1] John G. Julias,[1,2] W. Gregory Alvord,[3] Jangsuk Oh,[1] and Stephen H. Hughes[1]*

HIV Drug Resistance Program, National Cancer Institute at Frederick, Frederick, Maryland[1]; Basic Research Program, SAIC-Frederick, Inc., Frederick, Maryland[2]; and Data Management Services, National Cancer Institute at Frederick, Frederick, Maryland 21702-1201[3]

Received 2 May 2005/Accepted 3 August 2005

Retroviral polypurine tracts (PPTs) serve as primers for plus-strand DNA synthesis during reverse transcription. The generation and removal of the PPT primer requires specific cleavages by the RNase H activity of reverse transcriptases; removal of the PPT primer defines the left end of the linear viral DNA. We replaced the endogenous PPT from RSVP(A)Z, a replication-competent shuttle vector based on Rous sarcoma virus (RSV), with alternate retroviral PPTs and the duck hepatitis B virus "PPT." Viruses in which the endogenous RSV PPT was replaced with alternate PPTs had lower relative titers than the wild-type virus. 2-LTR circle junction analysis showed that the alternate PPTs caused significant decreases in the fraction of viral DNAs with complete (consensus) ends and significant increases in the insertion of part or all of the PPT at the 2-LTR circle junctions. The last two nucleotides in the 3′ end of the RSV PPT are GA. Examination of the (mis)cleavages of the alternate PPTs revealed preferential cleavages after GA dinucleotide sequences. Replacement of the terminal 3′ A of the RSV PPT with G caused a preferential miscleavage at a GA sequence spanning the PPT-U3 boundary, resulting in the deletion of the terminal adenine normally present at the 5′ end of the U3. A reciprocal G-to-A substitution at the 3′ end of the murine leukemia virus PPT increased the relative titer of the chimeric RSV-based virus and the fraction of consensus 2-LTR circle junctions.

Reverse transcription is catalyzed by the viral enzyme reverse transcriptase (RT). Retroviral RTs have two activities, a DNA polymerase that can copy both RNA and DNA templates and an RNase H that digests RNA if, and only if, it is hybridized to DNA. The RT of avian sarcoma leukosis viruses, of which Rous sarcoma virus (RSV) is a member, is found predominantly as a heterodimeric complex comprised of α and β subunits. The α subunit (63 kDa) contains the polymerase and RNase H domains, and the β subunit (95 kDa) contains both the polymerase and RNase H domains as well as the viral integrase. In the αβ heterodimeric complex, both the polymerase and the RNase H active sites are found in the α subunit (28).

During reverse transcription, cleavage of the RNA genome by RNase H is generally nonspecific; however, RNase H does make several specific cleavages involving the plus-strand and minus-strand RNA primers. One specific cleavage removes the tRNA primer used for minus-strand DNA synthesis, and this cleavage ultimately defines the right end of the linear viral DNA. Specific cleavages also generate (and remove) the polypurine tract (PPT) primer used for plus-strand DNA synthesis. Removal of the PPT primer defines the left end of the linear viral DNA. Thus, proper cleavage of the RNA primers generates the ends of the linear viral DNA that are the substrates for integration of the viral DNA into the host genome. More complete descriptions of reverse transcription and integration are given in the following reviews: references 20, 26, and 29.

The cleavage and the generation of the PPT plus-strand DNA primer by RNase H have been studied extensively. In order for the PPT primer to be specifically cleaved, the RNase H domain must be able to solve several problems. First, it must be able to distinguish an RNA-DNA duplex from an RNA-RNA and a DNA-DNA duplex and degrade the RNA only when it is in a complex with DNA. RT can make this distinction because RNA-RNA, RNA-DNA, and DNA-DNA duplexes differ in structure. RNA-RNA duplexes preferentially adopt an A-form structure in solution, while DNA-DNA duplexes preferentially adopt a B-form structure. The RNA-DNA duplex adopts a structure that is intermediate between the A and B forms, called the H-form (5).

The second problem encountered by the RT is how to distinguish the PPT (which should not be cleaved) from the rest of the RNA genome. RNase H does not recognize a specific sequence per se; rather, it appears that the structure of the RT/PPT complex allows RT to cleave the PPT specifically. Crystallographic studies of the structure of the human immunodeficiency virus type 1 (HIV-1) PPT (RNA/DNA) in a complex with RT provide a valuable framework for interpreting the biochemical data on RNase H cleavage. The HIV-1 PPT (5′-AAAAGAAAAGGGGGG-3′) has two stretches of adenine residues (A-tracts) at the 5′ end and a G-tract at the 3′ end.

* Corresponding author. Mailing address: HIV Drug Resistance Program, NCI-Frederick, P.O. Box B, Bldg. 539, Rm. 130A, Frederick, MD 21702-1201. Phone: (301) 846-1619. Fax: (301) 846-6966. E-mail: hughes@ncifcrf.gov.

The crystal structure of the RT/PPT complex shows that the minor groove of the PPT is relatively narrow and there is a bend in the AGA sequence that connects the two A-tracts. In addition, there are two weakly paired bases and two unpaired bases that cause a shift in the base pairing out of register and back into register (23). When the crystal structure of an unliganded HIV-1 PPT is compared to the structure of the HIV-1 RT/PPT complex, there is a bend at the AGA step, but the unpaired and mispaired bases are not present (12). However, chemical footprinting studies of the PPT (RNA-DNA hybrid) show that some of the template thymidines complementary to the adenines in the 5′ end of the HIV-1 PPT are susceptible to potassium permanganate modification, suggesting that the base pairing is weak (13). Taken together, these data suggest that this specific region of the PPT is malleable and can be deformed by interactions with the HIV-1 RT. The relatively narrow minor groove in the A-tract regions of the PPT in complex with HIV-1 RT is postulated to affect the trajectory of the nucleic acid substrate relative to the RNase H active site, contributing to the PPT's ability to resist RNase H cleavage (23). One of the factors that make this idea attractive is that the AGA step and polypurine tracts (A-tracts or G-tracts) found in the HIV-1 PPT are also present in other retroviral PPTs, including the RSV PPT.

The sequence of the PPT helps to determine the cleavage specificity of the RT/PPT complex, presumably because it affects the structure of the RT/PPT complex. Mutations in both the 5′ and 3′ ends of the HIV-1 PPT can affect the ability of HIV-1 RT to cleave specifically and reduce the viral titer (10, 15, 17). Mutating the second and fifth guanine residues (numbered from the PPT-U3 junction) of the G-tract at the PPT 3′ end had particularly strong effects on in vivo cleavage specificity and titer (10). These regions of the PPT are important in other retroviruses. In murine leukemia virus (MLV), a mutant that had nucleotide substitutions of the PPT upstream of the 3′ G-tract had delayed viral replication; a mutant in which the G-tract was replaced with other nucleotides had no measurable titer (21).

The polymerase and RNase H domains of HIV-1 RT make a number of contacts with nucleic acid substrates. The crystal structure of the HIV-1 RT/PPT complex revealed a network of amino acids adjacent to the RNase H active site, called the RNase H primer grip, that primarily contacts the sugar-phosphate backbone of the nucleic acid (23). Two of the amino acids in the RNase H primer grip, Y501 and Q475, play important roles in directing RNase H cleavage. A Y501A mutation affected the cleavage specificity of the HIV-1 RT (11), and mutating the equivalent residue in MLV RT decreased the fidelity of DNA synthesis (30). The contacts between Y501 and Q475 and the nucleic acid are thought to be important for positioning the primer strand relative to the RNase H and polymerase active sites.

Because cleavage specificity is affected by the structure of the RT/PPT complex, this suggests that a particular RT might show specificity for its cognate PPT. This type of specificity has been reported in in vitro experiments. MLV RT was unable to properly cleave the PPT primer in a RNA-DNA hybrid containing the RSV PPT sequence (14). However, MLV RT could properly cleave RNA-DNA hybrids containing the HIV-1 PPT sequence in plus-strand priming reactions (18), presumably because the MLV and HIV-1 PPT sequences are very similar. In addition, the avian myeloblastosis virus (AMV) RT preferentially miscleaved the RNA PPT primer of an RNA-DNA hybrid fragment containing the Moloney MLV PPT sequence at one position (4). Furthermore, neither HIV-1 RT nor human foamy virus RT was able to properly cleave PPTs from the other virus (3).

In this report we show that RSV can replicate when the endogenous PPT is replaced by PPTs from other retroviruses. However, the viral titers are decreased by the substitution mutations, and the cleavage specificity is altered. In addition, we show that, in contrast to the results obtained with the HIV-1 RT, RSV RT "recognizes" and preferentially cleaves after a GA dinucleotide sequence at the PPT-U3 junction.

MATERIALS AND METHODS

Cell line propagation. DF-1, a cell line derived from line EV-O chicken embryonic fibroblasts (7, 24), was grown in Dulbecco's modified Eagle's medium (GIBCO) supplemented with 5% newborn calf serum, 5% fetal bovine serum, 100 U of penicillin per ml, and 100 μg of streptomycin per ml (GIBCO) at 39°C. The cells were passaged at a 1:5 dilution for routine propagation.

Construction of RSVP(A)Z1-LTR*gfp* chimeric PPT mutants. The different PPTs were introduced into RSVP(A)Z (16) through a cloning scheme similar to the BspMI cloning strategy that has been previously described (15). Initially, an intermediate SapI cassette was generated in a modified pBluescript II KS(+) plasmid (Stratagene). The SapI cleavage site in the original plasmid was eliminated by QuikChange mutagenesis (Stratagene) using primers KCNAR-FOR (5′-CGGTTTGCGTATTGGGCGCCCTGCCGCTTCCTCGCTCACTG-3′) and KCNAR-REV (5′-CAGTGAGCGAGGAAGCGGCAGGGCGCCCAATACG CAAACCG-3′), and the mutation was confirmed by restriction digest analysis. The SapI cassette was built by cloning in three overlapping fragments, generated by PCR, that spanned the 2.1-kb ClaI-to-SacI fragment containing the PPT from RSVP(A)Z into pBluescript II KS(+) (SapI$^-$). The first PCR fragment included a segment from the ClaI site to the 5′ end of the PPT and was generated using the primers RCF (5′-TGTGGCATCGATACTAGTCGTACG-3′) and RCRevSapI (5′-GCATAAAGCTTGCGGCTCTTCGCGAAACTACTATATCCTAAG-3′). The second fragment included a segment from the AseI site to the 3′ end of the polypurine tract and was generated using the PCR primers RCFSapI (5′-GAA TAAAGCTTGCGGCTCTTCTGCAATACTCTTGTAGTCTTGC-3′) and AseRev (5′-GACTACATTAATGAAGCCTTCTG-3′). The third PCR fragment included a segment spanning the AseI site to the SacI site and was generated using the primers AseFor (5′-GGCTTCATTAATGTAGTCTTATGC-3′) and RSACRev (5′-GCCCCTATTTCCTTCTTAGAAGG-3′). A three-way ligation was then performed to clone the three fragments into pBluescript II KS(+) (SapI$^-$). The resulting SapI cassette introduced two SapI sites that flank the endogenous PPT. Complementary oligonucleotides (Fig. 1) that contained the different retroviral PPTs and duck hepatitis B virus "PPT-like" tracts were phosphorylated with polynucleotide kinase and annealed as previously described (15). The annealed oligonucleotides were then ligated into the SapI cassette using the two SapI restriction sites. The different PPTs in the SapI cassette were cloned into RSVP(A)Z using the MluI and SacI sites.

RSVP(A)Z was converted from a 2-LTR into a 1-LTR vector by digestion with PvuI and self-ligation. The gene for green fluorescent protein (GFP) was introduced into RSVP(A)Z by subcloning the *gfp* gene into the ClaI adapter plasmid, Cla12Nco (8), using NcoI and BamHI sites. The *gfp* gene was then cloned into the ClaI site of RSVP(A)Z1-LTR to generate RSVP(A)Z1-LTR*gfp*.

The YMDD mutant has a D-to-N substitution in the second aspartic acid of the conserved "YMDD motif" of the RT polymerase active site and was generated by QuikChange mutagenesis (Stratagene) using the primers RTACTFOR (5′-TATATGGACAATCTTTTGCTAGCCGCC-3′) and RTACTREV (5′-GG CGGCTAGCAAAAGATTGTCCAT-3′) and a template which had the HpaI-to-BspHI fragment from RSVP(A)Z subcloned into pBluescript II KS(+). The segment carrying this mutation was introduced into RSVP(A)Z1-LTR*gfp* using the HpaI and BspHI sites.

Virus production. Viral stocks were generated by calcium phosphate-mediated transfection of DF-1 cells seeded at 2×10^6 cells in 100-mm dishes (Falcon). Ten μg of the plasmids encoding the retroviral vectors were transfected into cells on 100-mm dishes for 4 h at 39°C. The transfected cells were subjected to glycerol shock for 3 min using culture medium supplemented with 15% sterile glycerol.

		Relative Titer
RSV PPT	5′-TCGCTTTTGCAT**AGGGAGGGGGA**AATGTAGTCTTAT-3′ 3′-GAAAACGTA**TCCCTCCCCCT**TTACATCAGAATACGT-5′	100%
MLV PPT	**AGAAAAAGGGGGG** **TCTTTTTCCCCCC**	32%
HIV-1 PPT	**AAAAGAAAAGGGGGG** **TTTTCTTTTCCCCCC**	26%
HFVLong PPT	**AGAGAGGAAGTAACGAGGAGAGGG** **TCTCTCCTTCATTGCTCCTCTCCC**	8%
HFVShort PPT	**AACGAGGAGAGGG** **TTGCTCCTCTCCC**	20%
SNVLong PPT	**GACCAGAACATACAAGAGCAGTGGGG** **CTGGTCTTGTATGTTCTCGTCACCCC**	11%
SNVShort PPT	**ACAAGAGCAGTGGGG** **TGTTCTCGTCACCCC**	13%
TY-1 PPT	**TGGGTGGTA** **ACCCACCAT**	8%
DuckHepB PPT	**TACATACACCCCTCTC** **ATGTATGTGGGGAGAG**	12%
DuckHepBFlip PPT	**GAGAGGGGTGTATGTA** **CTCTCCCCACATACAT**	38%
RSV PPT2	**AGGGAGGGGGG** **TCCCTCCCCCC**	73%
MLV PPT2	**AGAAAAAGGGGGA** **TCTTTTTCCCCCT**	61%
RSV(YMDD)	**AGGGAGGGGGA** **TCCCTCCCCCT**	ND

FIG. 1. Sequences of the PPT (bold) and flanking regions (nonbold) found in the chimeric PPT viruses and the relative titers of the viruses. In the mutant viruses, the sequences in bold are inserted into the RSV sequence between −12 and +1. Shown are the RSV, MLV, HIV-1, HFVLong, HFVShort, SNVLong, SNVShort, TY-1, DuckHepB, and DuckHepBFlip PPTs. The numbers above the RSV PPT designate the position of the nucleotide relative to the PPT-U3 junction. The relative titers were obtained by determining the titers of the viruses on 293-*tva* cells and normalizing the values to the amount of p27, as measured by p27 antigen-capture ELISA. The data are the averages of two independent experiments and were normalized to the value for a virus with a wild-type RSV PPT. The relative titer of the RSV(YMDD) mutant was not detectable (ND).

Following the glycerol shock, the cells were washed twice with 1× phosphate-buffered saline, and the normal culture medium was replaced. Two days post-transfection, supernatants were collected from the cells and clarified by low-speed centrifugation at 3,000 rpm for 15 min. The clarified supernatant was used to infect fresh DF-1 cells. The relative titer of the viral stocks was measured on a 293-*tva* cell line (a kind gift from John A. T. Young). The number of GFP-positive cells was determined by flow cytometry and normalized to the amount of p27 antigen present in the infecting viral stock. The amount of p27 antigen was measured by p27 antigen-capture enzyme-linked immunosorbent assay (ELISA) (2).

2-LTR circle junction analysis. DF-1 cells were seeded at 5×10^5 cells per 60-mm dish (Falcon) and infected overnight at 39°C with viral stocks, using the same amount of p27 in each infection. Two days postinfection, DNA was isolated from the cells using the EZ-1 DNA tissue protocol and the QIAGEN BioRobot. The 2-LTR circle junctions were amplified by PCR using the primers 2LTRFOR2 (5′-CGAACCACTGAATTCCGCATTGCAG-3′) and 2LTRREV2 (5′-ACCATTCTTCTAGACAATCCATGTCAGACCCGTCTGTTGC-3′), and the resulting PCR products were subcloned into pBluescript II KS(+) through the EcoRI and XbaI restriction sites introduced by the primers. DNA was isolated from the clones, and approximately 90 clones were sequenced for each mutant.

Statistical methods. The data were analyzed by log-linear categorical analysis, contingency table analysis, and related methods. I-by-J circle junction-by-mutant tables were decomposed through the use of likelihood ratio chi-square statistics into independent partitions to show associations between circle junction and/or mutant groupings and categories. Subsets of pertinent groupings were followed up with traditional two-by-two chi-square analyses and Fisher's exact tests.

RESULTS

Replacement of the endogenous Rous sarcoma virus PPT with other retroviral PPTs affects the viral titer. Previous studies have demonstrated that some retroviral reverse transcriptases have specificity for their cognate PPTs (4, 14). In the experiments reported here, we asked whether the vectors derived from RSV could replicate using PPTs from different retroviruses (and other viruses). The PPT from RSVP(A)Z (16), a replication-competent, RSV-based shuttle vector, was replaced with the PPT from other retroviruses and with a

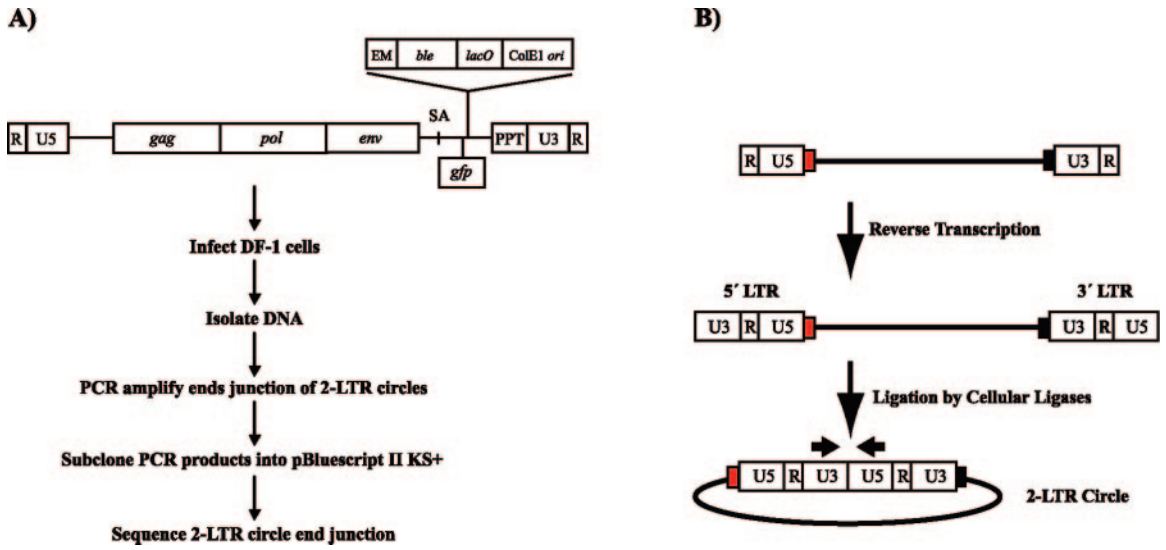

FIG. 2. (A) Viral RNA genome of RSVP(A)Z1-LTR*gfp* and the protocol for the 2-LTR circle junction assay. The virus encodes *gag*, *pol*, and *env*. A cassette that encodes the zeocin resistance gene (*ble*) under the control of the EM7 promoter (EM), the *lac* operator (*lacO*), and a ColE1 origin of replication (*ori*) was inserted between the splice acceptor (SA) and the PPT. The *gfp* gene was inserted downstream of the SA and is expressed under the control of the viral LTR. (B) Generation of the 2-LTR circle junctions. During infection, the single-stranded RNA genome is converted to double-stranded DNA by reverse transcription. Some of the linear viral DNAs are ligated by cellular enzymes to generate 2-LTR circles. The figure shows the viral LTRs, tRNA (red box), and PPT (black box). The arrows above U3 and U5 show the positions and directions of the primers used to PCR amplify the junctions of the 2-LTR circles.

"PPT-like" sequence from the duck hepatitis B virus (Fig. 1). RSVP(A)Z was converted into a 1-LTR viral vector by digestion with PvuI and self-ligation. This modification ensured that, if there were any plasmid carry-over into the infected cells, it would not affect the analyses of the 2-LTR circle junctions. The modified vector, RSVP(A)Z1-LTR, replicated as well as the 2-LTR parental vector based on monitoring reverse transcriptase activity (data not shown). This is the expected result, because both vectors should give rise to identical viral RNA genomes. The vector was further modified by inserting the *gfp* gene into the ClaI site, immediately upstream of the zeocin cassette, to simplify determination of the titer of the virus. This places GFP expression under the control of the LTR. The insertion of the *gfp* gene immediately upstream of the zeocin cassette disrupts the expression of the zeocin resistance gene (*ble*) in mammalian cells, but not in prokaryotes. In prokaryotes, *ble* is expressed from the EM7 promoter in the cassette. A schematic of the viral vector is shown in Fig. 2A. Because retroviruses have high mutation rates, the viral stocks used for infections were generated by transfection with the viral vectors. Viral titers were measured in 293-*tva* cells, and the number of GFP-expressing cells was determined by flow cytometry. The relative titer was determined by normalizing the viral titer to the amount of p27 antigen in the viral stock used to infect the 293-*tva* cells, measured by p27 antigen-capture ELISA. These values were then normalized to wild type.

Replacing the endogenous RSV PPT with other retroviral PPTs reduced the relative titer. Chimeric PPT mutants containing the MLV, HIV-1, and a truncated version of the human foamy virus (HFVShort) PPT had relative titers (corrected for the amount of p27) ranging from 32% to 20% of the wild-type RSVP(A)Z1-LTR*gfp* virus (Fig. 1). The duck hepatitis B virus PPT in reverse orientation (DuckHepBFlip PPT) had a relative titer of 38%. Replacement of the endogenous PPT with the spleen necrosis virus full-length (SNVLong PPT) and a shortened SNV PPT (SNVShort PPT), or duck hepatitis B virus "PPT" (DuckHepB PPT) reduced the titer to 11% to 13%. Further reductions in the relative titer were seen with the full-length human foamy virus PPT (HFVLong PPT) and the yeast retrotransposon, TY-1 PPT (TY-1 PPT) chimeric PPT viruses, both of which had relative titers of 8%. RSV(YMDD), the negative control that has an inactivating mutation in the conserved YMDD motif at the polymerase active site of RSV RT, had no measurable titer.

Our initial experiments with the alternate PPTs suggested that the adenine that is the 3′-most nucleotide in the wild-type RSV PPT could have an important role in directing RNase H cleavage (data not shown). To test this hypothesis, the adenine in the RSV PPT was mutated to guanine by site-directed mutagenesis (RSV PPT2). This mutation makes the 3′ end of the RSV PPT similar to the MLV and HIV-1 PPTs (Fig. 1). In addition, a reciprocal mutation was made in the MLV PPT, replacing the 3′-most nucleotide in the PPT (a guanine) with an adenine (MLV PPT2) (Fig. 1). The A-to-G substitution of the RSV PPT decreased the relative titer of the virus to 73% compared to wild type (Fig. 1). The G-to-A substitution of the MLV PPT (MLV PPT2) increased the relative titer nearly twofold, from 32% to 61% (Fig. 1). When we compared the amount of p27 produced by infected cells 2 days after infection using p27 antigen-capture ELISA, the results were similar, but not identical, to the relative titer of the viral stocks (data not shown).

2-LTR circle junction analysis of chimeric PPT viruses. The majority of the linear double-stranded retroviral DNAs in cells infected with wild-type viruses will become properly inte-

A)

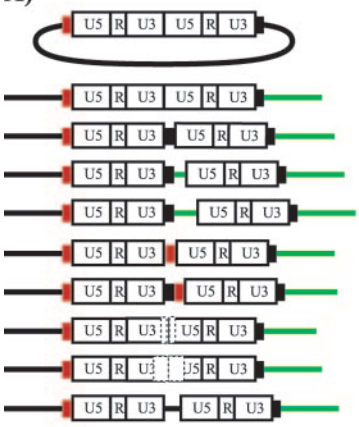

2-LTR Circle Junctions	RSV PPTA1	RSV PPTA2	RSV PPTB	RSV PPTC
Consensus	0.62	0.54	0.50	0.64
Simple PPT insert	0	0.04	0.06	0.04
PPT+short flank insert	0	0	0	0
PPT+long flank insert	0.01	0.01	0.01	0.01
tRNA insert	0.09	0.07	0.10	0.04
tRNA + PPT insert	0	0	0.01	0
Small deletion	0.05	0.08	0.06	0.08
Large deletion	0.23	0.24	0.26	0.18
Insertion	0	0.02	0	0.01

B)

2-LTR Circle Junctions	RSV PPT	MLV	HIV-1	HFVLong	HFVShort	SNVLong	SNVShort	DuckHepBFlip	RSV PPT2	MLV PPT2
Consensus	0.59	0.13	0.10	0.29	0.18	0.18	0.04	0	0.22	0.26
Simple PPT insert	0.04	0.36	0.45	0.15	0.32	0.12	0.57	0.80	0.11	0.16
PPT+short flank insert	0	0	0.01	0	0	0.01	0	0	0	0
PPT+long flank insert	0.01	0.01	0	0.06	0.03	0.06	0.04	0.02	0.02	0.02
tRNA insert	0.05	0.11	0.07	0.10	0.03	0.07	0.04	0	0.07	0.11
tRNA + PPT insert	0	0.03	0.01	0.01	0	0	0.07	0.01	0.04	0.01
Small deletion	0.08	0.11	0.22	0.31	0.25	0.24	0.05	0.01	0.28	0.09
Large deletion	0.21	0.23	0.15	0.04	0.20	0.31	0.17	0.15	0.25	0.35
Insertion	0.02	0.01	0	0.04	0	0.01	0.01	0.01	0.01	0

FIG. 3. 2-LTR circle junctions produced by PPT mutants. (A) Schematic representation of the mutations found in the 2-LTR circle junction analysis and relative amounts of the consensus and aberrant sequences found at the circle junctions of wild-type-infected samples. Depicted are insertions of the tRNA (red box), PPT (black box), and upstream sequences flanking the PPT (green line). Consensus sequences represent the joining of the correct ends of the linear viral DNA. Simple PPT insert mutations ranged from one nucleotide to the entire polypurine tract inserted into either a consensus sequence junction or into a junction with a deletion in U5. PPT + short flank inserts were insertions of the PPT with no more than 10 nucleotides from the segment immediately upstream of the PPT. The PPT + long flank inserts were identical to the PPT + short flank inserts except that the mutations contained more than 10 nucleotides from the flanking region immediately upstream of the PPT. The tRNA inserts consisted of one or more nucleotides from the tryptophan tRNA primer inserted at the circle junction. The tRNA + PPT inserts were the same as the tRNA inserts except they also contained either a portion of, or the entire, PPT. Small deletion mutants had deletions of no more than 10 nucleotides in the U5 and/or U3. Large deletion mutants had deletions larger than 10 nucleotides in the U5 and/or U3. Insertion mutants had nucleotide insertions from sequences other than from the polypurine tract or tRNA at the circle junction. In the cases where there were both insertions of nucleotides not derived from the PPT or tRNA and deletions of either U5 and/or U3, the mutants were classified based on which mutation involved more nucleotides. (B) Fractions of consensus and mutant sequences found at the ends of the 2-LTR circle junctions in wild-type (RSV PPT) and chimeric PPT virus-infected samples. The data represent the average of two independent experiments.

grated. However, a portion of the linear viral DNAs that are not integrated can be ligated by cellular enzymes to form 2-LTR circles (Fig. 2B). As has already been discussed, the ends of the linear viral DNAs are generated by specific cleavages that remove the tRNA primer and cleavages that generate and remove the PPT primer. Integration preferentially involves linear DNAs with correct (consensus) ends. Linear viral DNAs with aberrant ends can be monitored by analyzing the junction sequences in 2-LTR circles.

DF-1 cells, an avian fibroblast cell line, were infected with wild-type and the chimeric PPT viruses. DNA was prepared from lysates of the infected cells 2 days postinfection. 2-LTR circle junctions were amplified using PCR primers that introduced XbaI and EcoRI sites into the PCR products (Fig. 2B), and the fragments were subcloned into pBluescript II KS(+). For each mutant, approximately 90 clones were sequenced and analyzed. A schematic outline of the protocol is shown in Fig. 2A. Two experiments were performed with the wild-type RSVP(A)Z1-LTR*gfp* virus, RSV PPTA1 and RSV PPTA2, in which the same infected cell lysate was amplified in two separate PCRs (Fig. 3A). Two additional experiments were performed with samples derived from two independent infections with the wild-type RSVP(A)Z1-LTR*gfp* virus to determine the reproducibility of the assay; the results are given in Fig. 3A (RSV PPTB and RSV PPTC). The percentages of consensus sequences (representing the ligation of a linear DNA with correct 3′ and 5′ ends) and the various classes of aberrant junctions found in the four experiments, RSV PPTA1, RSV PPTA2, RSV PPTB, and RSV PPTC, were not significantly different by chi-square analysis ($P = 0.865$). The P values shown are the results of chi-square analyses unless otherwise stated.

2-LTR circle junction analysis of the chimeric PPT mutants

revealed differences in the number of consensus sequences, small deletions of U5 and/or U3, and in the retention of part or all of the PPT (simple PPT insert) when compared to wild type (Fig. 3B). We were not able to amplify 2-LTR circle junctions from samples infected with the RSV(YMDD) mutant, the DuckHepB PPT, or the TY-1 PPT chimeric viruses using the PCR conditions described in Material and Methods. Replacing the endogenous RSV PPT with alternate retroviral PPTs significantly decreased the amount of consensus 2-LTR circle junctions with all the chimeric PPT viruses. Strikingly, no consensus sequences were detected in DuckHepBFlip PPT-infected samples (Fig. 3B), even though the relative titer was 38% of wild type (Fig. 1). Introducing an A-to-G substitution in the RSV PPT2 mutant significantly decreased the amount of consensus 2-LTR circle junctions more than twofold, from 59% to 22% ($P < 0.0001$), compared to wild type. The G-to-A substitution of the MLV PPT (MLV PPT2) significantly increased the number of consensus 2-LTR circle junctions by twofold (from 13% to 26%; $P = 0.005$), compared to the MLV PPT.

In comparison to wild type, there were significant increases in the number of 2-LTR circle junctions with small deletions of the U5 and/or U3 (10 nucleotides or less) from samples infected with the HIV-1 PPT ($P = 0.0007$), HFVLong PPT ($P < 0.0001$), HFVShort PPT ($P < 0.0001$), SNVLong PPT ($P < 0.0001$), and RSV PPT2 ($P < 0.0001$) mutant viruses and a significant decrease with the DuckHepBFlip PPT ($P = 0.0018$; Fisher's exact test). The percentage of large deletions (11 nucleotides or more) in the U5 and/or U3 was comparable to wild type for most of the chimeric PPT mutants. However, there was a significant decrease in the percentage of large deletions in the 2-LTR circle junctions from infections with the HFVLong PPT chimeric virus ($P < 0.0001$), and a significant increase with the MLV PPT2 mutant ($P = 0.008$).

Significant increases of simple PPT inserts (the result of miscleaving either in the generation of the PPT primer or its removal) were seen with all of the chimeric PPT mutants, compared to wild type. Four percent of the 2-LTR circle junction sequences derived from wild-type-infected samples had simple PPT inserts; however, samples from the MLV PPT or HIV-1 PPT chimeric viruses showed a 9-fold (36%; $P < 0.0001$) and 11-fold increase (45%; $P < 0.0001$), respectively, in PPT insertions compared to wild type. In addition, 57% of the sequences analyzed from SNVShort PPT-infected samples ($P < 0.0001$) and 80% of the sequences from DuckHepBFlip PPT-infected samples ($P < 0.0001$) had simple PPT inserts (Fig. 3B). The presence or absence of an A at the 3′ end of the PPT affected the percentage of retained PPT sequences. The percentage of simple PPT inserts increased more than twofold for the RSV PPT2 mutant ($P = 0.009$) compared to wild type, whereas the percentage of simple PPT inserts decreased from 36% (MLV PPT) to 16% for the MLV PPT2 mutant ($P = 0.0001$) (Fig. 3B).

The length of the PPT had an effect on the sequences found at the 2-LTR circle junctions. Circle junctions obtained from cells infected with the HFVLong PPT and SNVLong PPT mutant viruses and with viruses encoding truncated versions of the PPTs (HFVShort and SNVShort) showed that there were significant differences in the percentage of consensus sequences and simple PPT inserts between the full-length and shortened versions of the PPTs. Truncating the HFV and SNV PPTs to a length similar to the endogenous RSV PPT decreased the percentage of consensus sequences and increased the percentage of simple PPT inserts. Depending on the PPT, opposite effects were seen when the percentages of large deletion mutations were compared for the full-length and truncated PPTs. Truncating the HFV PPT significantly increased the percentage of large deletions ($P < 0.0001$), whereas truncating the SNV PPT significantly decreased the number of large deletions ($P = 0.0024$) (Fig. 3B). The relative titer increased 2.5-fold when the full-length HFV PPT was truncated; however, the relative titers for the mutant viruses encoding the full-length and truncated versions of the SNV PPT were essentially equivalent (Fig. 1). The larger fraction of consensus sequences seen for the full-length PPTs compared to the truncated versions could be due to the fact that the 2-LTR circle assay only amplifies reverse transcription products that are essentially complete. The full-length HFV and SNV PPTs may be too "foreign" for the RSV RT to allow for efficient completion of reverse transcription. However, the viral DNAs for which reverse transcription is complete or nearly complete have mostly consensus sequences.

RSV RNase H cleavage specificity of the alternate PPTs and RSV PPT2. The substitution of the endogenous RSV PPT with other viral PPTs affected the specificity of RNase H cleavage. Although the wild-type PPT was occasionally miscleaved by the RNase H, these miscleavages did not appear to strongly favor a specific position near the RSV PPT-U3 border (Fig. 4). However, some of the alternate PPTs were miscleaved by the RSV RT in specific, reproducible patterns. Two separate experiments were done, and the two sets of data are compared in Fig. 4. In the case of the MLV, HIV-1, and HFVShort PPTs, all of which contain a continuous 3′ G-tract, the RSV RT consistently miscleaved in a way that resulted in the insertion of one G. The relative frequency of the insertion of two Gs was roughly half the frequency of one G insertions (Fig. 4). Miscleavages that removed the first adenine residue in U3 immediately adjacent to the PPT were also favored in these chimeric PPT viruses.

The two nucleotides at the 3′ end of the RSV PPT are GA. The data obtained with the PPT substitutions suggest that the RNase H of the RSV RT prefers to cleave just 3′ of a GA dinucleotide in a purine-rich region. The pattern of (mis)cleavages for the RSV PPT2 (A-to-G substitution) mutant showed a strong preference for a deletion of the first adenine nucleotide in U3, whereas the wild-type RSV PPT was not preferentially cleaved at this (or any other) position (Fig. 4). The A-to-G substitution in RSV PPT2 shifted cleavage by one nucleotide. This shift allowed the RSV RNase H to cleave following a GA dinucleotide sequence. As mentioned above, a preferred site of miscleavage seen with the MLV, HIV-1, HFVShort, HFVLong, and SNVShort PPT mutant viruses removed the first A of U3. In all five cases, the RNase H cleavage occurred after a GA sequence. Introducing an A into the 3′ end of the MLV PPT (MLV PPT2) altered the cleavage pattern at the PPT-U3 junction from that seen with the MLV PPT virus (Fig. 4). The percentage of consensus sequences found with MLV PPT2 increased twofold compared to the MLV PPT virus (Fig. 3B), presumably because RNase H was able to recognize and cleave right after the newly created GA at the 3′

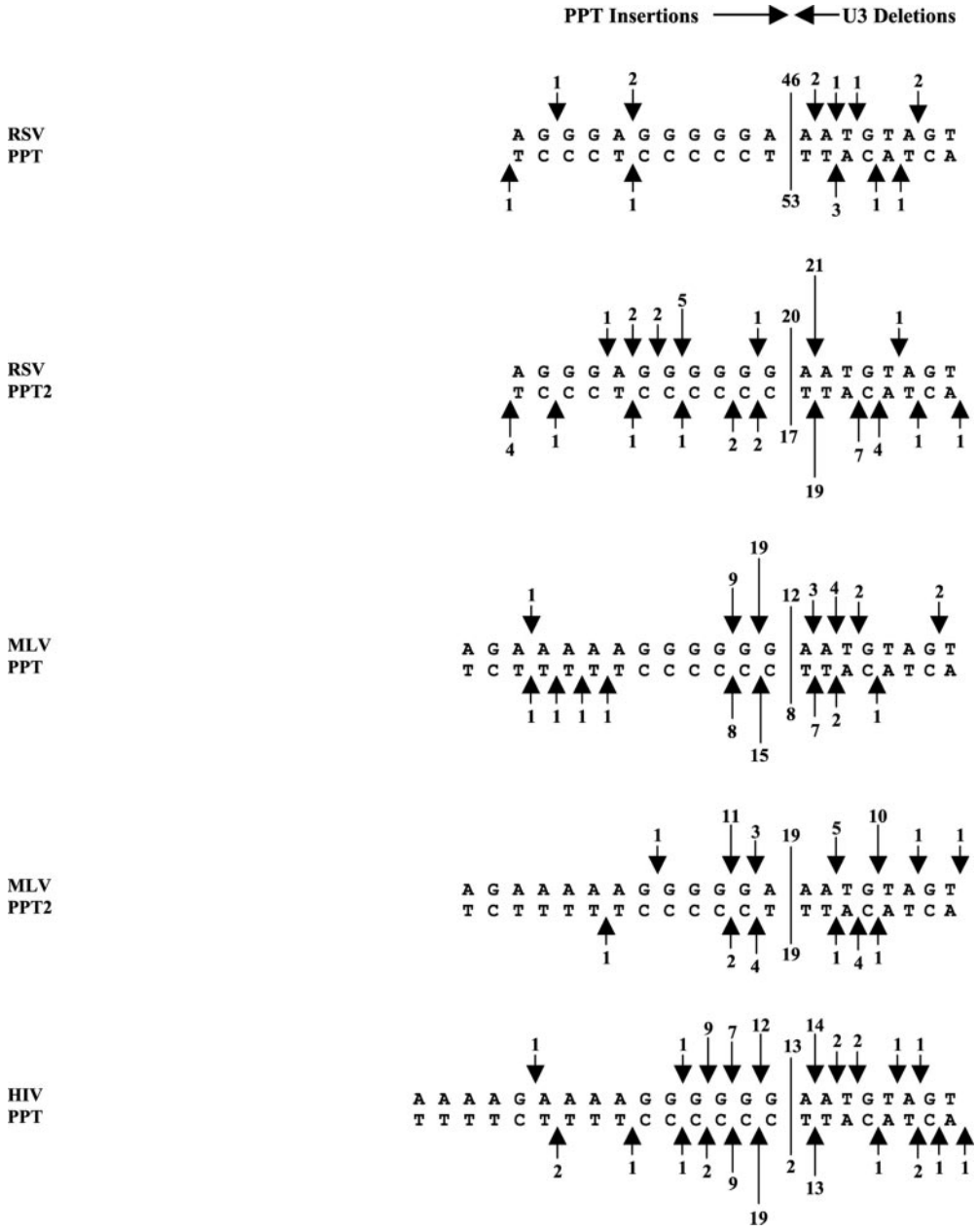

FIG. 4. Miscleavages of the wild-type and alternate PPTs by the RSV RT at the PPT-U3 junction. The arrows depict the positions of the PPT miscleavages, which result in insertions of part or all of the PPT (simple PPT inserts) or small deletions of the U3. The arrows at the top represent the results from one experiment, and the arrows at the bottom represent the results from a second, independent experiment. The size of the arrows is related to the number of events (denoted by a number above the arrow). The line delineates the border between the PPT and the U3, and the numbers above and below the line are the number of consensus sequences found in each experiment.

end of the PPT in MLV PPT2. Preferential miscleavages in the PPT following GA dinucleotide sequences were obvious with the HFVLong PPT virus (Fig. 4). The pattern of miscleavages seen with the full-length and truncated versions of the HFV and SNV PPTs differed, suggesting that the length of the PPT can also affect the RSV RNase H cleavage specificity.

The DuckHepBFlip PPT was miscleaved almost exclusively at one specific position within the PPT, resulting in the insertion of ATGTA (Fig. 4). The preference for this site was strong; no consensus sequences were detected in samples infected with this virus (Fig. 4). It is interesting that the ATGTA in the DuckHepBFlip PPT is a duplication of the 5′ end of the RSV U3, positions +2 to +6. This may explain the viruses' ability to recognize this DuckHepBFlip PPT and specifically miscleave at this particular site.

DISCUSSION

Retroviral PPTs are used to prime plus-strand DNA synthesis during reverse transcription. This requires specific RNase H cleavages to generate and remove the PPT primer. A key part of the cleavage specificity may lie in the unique structure of the

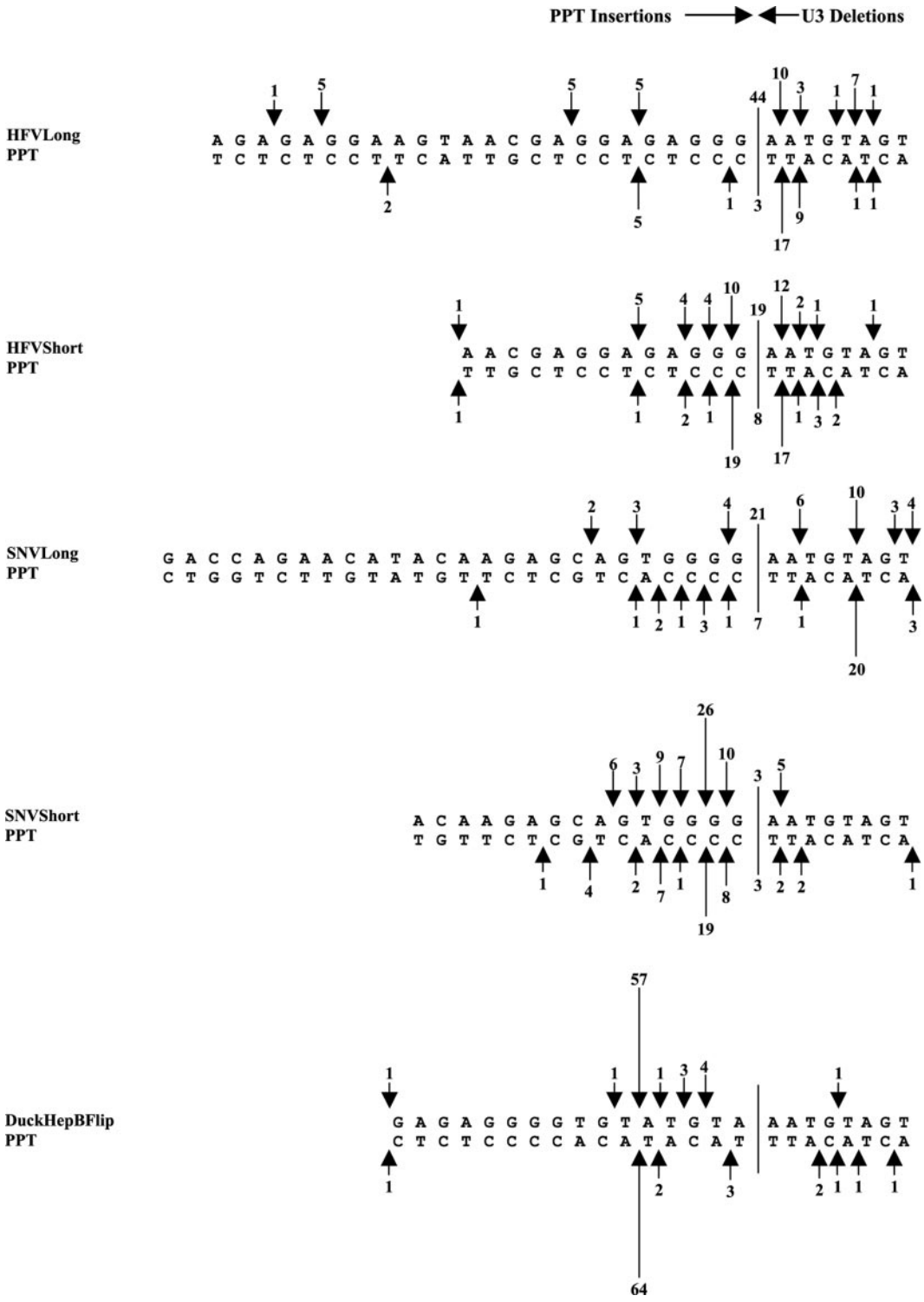

FIG. 4—*Continued.*

PPT. There are conserved sequence elements within retroviral PPTs and in the U-tract (1, 9, 21) that lies just upstream of the PPT, which influence the specific cleavage of the PPT by RT. This suggests that the process by which the various retroviral RTs specifically cleave their cognate PPTs share certain similarities. However, studies have also shown that there is specificity between a particular RT and its cognate PPT (4, 14, 19). In this report, we replaced the endogenous PPT of RSV with the PPT from other retroviruses and a polypurine tract derived from the duck hepatitis B virus and examined the ability of the RSV RT to recognize and properly utilize the foreign PPTs for viral replication.

Replacement of the endogenous PPT with alternate PPTs reduced the relative titer compared to the wild type; however, only the RT active site (YMDD) mutant had no measurable titer on 293-*tva* cells (Fig. 1). The YMDD motif is comprised of highly conserved amino acid residues in the polymerase active site of RT and is involved in the coordination of the metal ions found in the active site. Mutating one of the essential aspartic acid residues should block viral DNA synthesis completely. No PCR products were detected for the YMDD mutant in the 2-LTR circle junction assay suggesting that there was little or no reverse transcription. The primers used to amplify the 2-LTR circle junctions bind to the U5 of one LTR and the U3 of the other (Fig. 2B). Because our infections were initiated with a 1-LTR plasmid, the only way to generate 2-LTR circles (and PCR products) is if reverse transcription goes to completion, generating a complete linear viral DNA, and the ends of the DNA are ligated by cellular enzymes. PCR products were not detected for the TY-1 PPT or the DuckHepB PPT chimeric viruses; however, low titers were seen in 293-*tva* cells. Because the YMDD mutant had no detectable titer, this suggests that these viruses may be able to carry out sufficient reverse transcription to generate a detectable GFP signal, and the low-level GFP expression might arise from unintegrated and/or incomplete viral DNA. Our inability to amplify 2-LTR circle junctions by PCR suggests that these mutants synthesize little full-length linear viral DNA.

Replacement of the endogenous RSV PPT with alternate PPTs significantly decreased the percentage of consensus sequences and significantly increased the percentage of simple PPT inserts relative to wild type (Fig. 3B). This demonstrates that the sequence of the PPT influences the cleavage specificity of the RSV RT, as has been shown for other retroviruses. Analysis of the (mis)cleavages found at the PPT-U3 junction suggests that the RSV RT recognizes a GA dinucleotide sequence at the 3′ end of the PPT for specific cleavage of the PPT-U3 junction. A-to-G substitution of the −1 adenine residue in the RSV PPT (RSV PPT2) induced a preferential miscleavage by the RSV RT, resulting in the deletion of the +1 adenine residue found in U3 (Fig. 4). This preferred miscleavage directly follows a GA dinucleotide sequence. The (mis) cleavage following the +1 adenine residue is also seen when the RSV RT cleaves the HIV-1, HFVLong, HFVShort, SNVShort, and MLV PPTs. A similar result was obtained when the AMV RT cleaved an RNA-DNA hybrid containing the Moloney MLV PPT sequence in vitro. In those experiments, approximately two-thirds of the RNA PPT primers generated by the AMV RT retained an extra adenine residue that was adjacent to the terminal G at the 3′ end of the MLV PPT (4). G-to-A substitution of the −1 guanine residue in the MLV PPT (MLV PPT2) eliminated the preferred miscleavage of the +1 adenine and increased both the percentage of consensus 2-LTR circle junction sequences and relative titer of the virus about twofold. Miscleavages within the chimeric PPTs following GA dinucleotide sequences could also be seen with the HFVLong PPT and HFVShort PPT mutant viruses.

In the HIV-1 system, an analogous G-to-A substitution of the HIV-1 PPT 3′-end guanine residue did not affect the ability of the HIV-1 RT to properly cleave the PPT; neither the titer of the mutant viral vector nor the percentages of aberrant circle junctions differed from wild type (10). Furthermore, a MLV virus with a G-to-C substitution at the 3′ end of the wild-type MLV PPT showed modest delays in replication (22). This recognition of the GA dinucleotide sequence at the 3′ end of the PPT by RSV (or AMV) RT and the effects of altering the A residue on the cleavage of the PPT-U3 junction suggest that the way RSV RT recognizes its PPT differs from the ways in which HIV-1 and MLV RTs recognize their PPTs.

In vitro studies of the structure of the HIV-1 PPT as an RNA/DNA hybrid free in solution revealed that the T at the 5′ end of U3, immediately adjacent to the 3′ end of the PPT, was susceptible to potassium permanganate modification, indicating that the A-T base pair at that position was weakly base paired or distorted. The entire PPT was proposed to contribute to the distortion at +1, and there was a correlation between the precise cleavage of the PPT-U3 junction and the +1 distortion (13). If there were a similar weak pairing or distortion in the A-T base pair at the 3′ end of the RSV PPT, this could serve as a structural landmark for the RSV RT and/or affect the interaction of that portion of the PPT, making the base immediately following the GA dinucleotide particularly accessible to the active site of the RSV RNase H.

The length of the alternate PPTs also affected the RSV RNase H cleavage specificity. Truncating the HFVLong and SNVLong PPT (HFVShort and SNVShort, respectively) affected the percentages of consensus circle junction and aberrant circle junction sequences. The percentage of simple PPT inserts increased significantly when the HFV ($P = 0.0005$) and SNV ($P < 0.0001$) PPTs were truncated, compared to the full-length PPT encoding viruses, and were comparable to or higher than the percentages of simple PPT inserts seen with the MLV and HIV-1 PPT chimeric viruses. The length of the HFVShort PPT (13 nucleotides) and SNVShort PPT (15 nucleotides) are the same as the MLV PPT (13 nucleotides) and HIV-1 PPT (15 nucleotides), respectively. The (mis)cleavage patterns for the full-length and truncated version of the HFV and SNV PPTs also differed. The change in cleavage specificity seen between full-length and truncated PPT virus-infected samples could be due to an effect on the positioning of either the polymerase and/or RNase H active sites of RT relative to the nucleic acid substrate. Mutations in the polymerase domain of RT can influence the activity of the RNase H domain, including cleavage specificity, and in a similar sense mutations in RNase H can affect the activity of the polymerase (6, 25, 27, 31).

We were initially surprised by the ability of the virus carrying the DuckHepBFlip PPT to replicate and the RSV RT's (and RSV integrase's) ability to use the nucleic acids carrying this substitution mutation. The relative titer of the mutant virus encoding this PPT was higher than most of the other chimeric PPT viruses; however, no consensus sequences were detected in the 2-LTR circle junction analysis with the DuckHepBFlip PPT (Fig. 3B). The RSV RT (mis)cleaved the DuckHepBFlip PPT almost exclusively at one position, leaving an insertion of ATGTA (Fig. 4). This is an exact duplication of the 5′ end of the U3 (positions +2 to +6), and the cleavage data suggest that, in this mutant, the RSV RT recognizes that position as the PPT-U3 junction.

The remainder of the DuckHepBFlip PPT upstream of the ATGTA is the same length as the normal RSV PPT (11 nucleotides) and is, except for two Ts, purine rich. A GT dinu-

cleotide, which the RSV RNase H may accept as being similar to the GA at the 3′ end of the RSV PPT, is immediately upstream of the ATGTA. This may explain the ability of the RSV RNase H to (mis)cleave specifically at this particular position in the DuckHepBFlip PPT. The GT dinucleotide is part of a G-tract which, although not perfectly continuous, comprises the 3′ end of the remainder of the DuckHepBFlip PPT. This G-tract at the 3′ end of the DuckHepBFlip PPT is similar to what is found in most of the retroviral PPTs used in this study. In HIV-1, in vitro assays showed that the G-tract sequence found at the 3′ end of the PPT was sufficient for proper cleavage and processing of the PPT and priming of plus-strand DNA synthesis (17). However, in vivo analysis showed that mutations in the upstream A-rich region also affected the specificity of HIV-1 RNase H cleavage (15). In MLV, no measurable replication was detected for a mutant virus where the entire G-tract at the 3′ end of the PPT was mutated to other bases, whereas replication was delayed in a mutant virus that had the remainder of the PPT and several nucleotides upstream of the PPT mutated (21). These data suggest that the stretch of Gs found in the DuckHepBFlip PPT immediately upstream of the ATGTA may be sufficient to allow priming of plus-strand synthesis. The accidental similarities of the DuckHepBFlip PPT and the RSV PPT could explain how the RSV RT is able to cleave the DuckHepBFlip PPT in such a specific manner and prime plus-strand DNA synthesis. The ATGTA "insertion" seen with the DuckHepBFlip PPT virus may also explain the observation that the viral DNA apparently can undergo reasonably efficient integration, explaining the relatively high titer of this mutant virus. The ATGTA is a duplication of the 5′ end of U3 (+2 to +6), and a CA dinucleotide that could be used for integration is present. Although this CA is one nucleotide from the end of the linear viral DNA rather than the normal two nucleotides, it is possible that the integrase can still use this CA. Presumably, RSV integrase would not efficiently use the "normal" CA in U3, which is seven nucleotides from the left end of the DuckHepBFlip linear DNA.

These results highlight the differences in the way the RSV RT recognizes and processes its cognate PPT versus other PPTs, and they provide further in vivo evidence of the specificity of some RTs for their cognate PPT. In addition, the data obtained with the DuckHepBFlip PPT chimeric virus have helped elucidate the requirements for cleavage specificity by the RNase H of RSV RT and could provide useful information on the ability of RSV integrase to process aberrant linear viral DNA with inserts on the ends.

ACKNOWLEDGMENTS

We thank Stanislaw Kaczmarczyk for help with the p27 antigen-capture ELISA. We thank Refika Turnier for analyzing the fluorescence-activated cell sorter samples and the Laboratory of Molecular Technology for DNA sequencing. We also thank Hilda Marusiodis for help in preparation of the manuscript.

The research described in this publication was funded in part with federal funds from the National Cancer Institute, National Institutes of Health, under contract NO1-CO-12400, and by the Intramural Research Program of the NIH, National Cancer Institute, Center for Cancer Research.

The content of this publication does not necessarily reflect the views or policies of the Department of Health and Human Services, nor does mention of trade names, commercial products, or organizations imply endorsement by the U.S. Government.

REFERENCES

1. **Bacharach, E., J. Gonsky, D. Lim, and S. P. Goff.** 2000. Deletion of a short, untranslated region adjacent to the polypurine tract in Moloney murine leukemia virus leads to formation of aberrant 5′ plus-strand DNA ends in vivo. J. Virol. **74:**4755–4764.
2. **Barsov, E. V., W. S. Payne, and S. H. Hughes.** 2001. Adaptation of chimeric retroviruses in vitro and in vivo: isolation of avian retroviral vectors with extended host range. J. Virol. **75:**4973–4983.
3. **Boyer, P. L., C. R. Stenbak, P. K. Clark, M. L. Linial, and S. H. Hughes.** 2004. Characterization of the polymerase and RNase H activities of human foamy virus reverse transcriptase. J. Virol. **78:**6112–6121.
4. **Champoux, J. J., E. Gilboa, and D. Baltimore.** 1984. Mechanism of RNA primer removal by the RNase H activity of avian myeloblastosis virus reverse transcriptase. J. Virol. **49:**686–691.
5. **Fedoroff, O. Y., M. Salazar, and B. R. Reid.** 1993. Structure of a DNA:RNA hybrid duplex. Why RNase H does not cleave pure RNA. J. Mol. Biol. **233:**509–523.
6. **Gao, H.-Q., P. L. Boyer, E. Arnold, and S. H. Hughes.** 1998. Effects of mutations in the polymerase domain on the polymerase, RNase H and strand transfer activities of human immunodeficiency virus type 1 reverse transcriptase. J. Mol. Biol. **277:**559–572.
7. **Himly, M., D. N. Foster, I. Bottoli, J. S. Iacovoni, and P. K. Vogt.** 1998. The DF-1 chicken fibroblast cell line: transformation induced by diverse oncogenes and cell death resulting from infection by avian leukosis viruses. Virology **248:**295–304.
8. **Hughes, S. H., J. J. Greenhouse, C. J. Petropoulos, and P. Sutrave.** 1987. Adaptor plasmids simplify the insertion of foreign DNA into helper-independent retroviral vectors. J. Virol. **61:**3004–3012.
9. **Ilyinskii, P. O., and R. C. Desrosiers.** 1998. Identification of a sequence element immediately upstream of the polypurine tract that is essential for replication of simian immunodeficiency virus. EMBO J. **17:**3766–3774.
10. **Julias, J. G., M. J. McWilliams, S. G. Sarafianos, W. G. Alvord, E. Arnold, and S. H. Hughes.** 2004. Effects of mutations in the G tract of the human immunodeficiency virus type 1 polypurine tract on virus replication and RNase H cleavage. J. Virol. **78:**13315–13324.
11. **Julias, J. G., M. J. McWilliams, S. G. Sarafianos, E. Arnold, and S. H. Hughes.** 2002. Mutations in the RNase H domain of HIV-1 reverse transcriptase affect the initiation of DNA synthesis and the specificity of RNase H cleavage in vivo. Proc. Natl. Acad. Sci. USA **99:**9515–9520.
12. **Kopka, M. L., L. Lavelle, H. G. Won, H.-L. Ng, and R. E. Dickerson.** 2003. An unusual sugar conformation in the structure of an RNA/DNA decamer of the polypurine tract may affect recognition by RNase H. J. Mol. Biol. **334:**653–665.
13. **Kvaratskhelia, M., S. R. Budihas, and S. F. J. Le Grice.** 2002. Pre-existing distortions in nucleic acid structure aid polypurine tract selection by HIV-1 reverse transcriptase. J. Biol. Chem. **277:**16689–16696.
14. **Luo, G., L. Sharmeen, and J. Taylor.** 1990. Specificities involved in the initiation of retroviral plus-strand DNA. J. Virol. **64:**592–597.
15. **McWilliams, M. J., J. G. Julias, S. G. Sarafianos, W. G. Alvord, E. Arnold, and S. H. Hughes.** 2003. Mutations in the 5′ end of the human immunodeficiency virus type 1 polypurine tract affect RNase H cleavage specificity and virus titer. J. Virol. **77:**11150–11157.
16. **Oh, J., J. G. Julias, A. L. Ferris, and S. H. Hughes.** 2002. Construction and characterization of a replication-competent retroviral shuttle vector plasmid. J. Virol. **76:**1762–1768.
17. **Powell, M. D., and J. G. Levin.** 1996. Sequence and structural determinants required for priming of plus-strand DNA synthesis by the human immunodeficiency virus type 1 polypurine tract. J. Virol. **70:**5288–5296.
18. **Pullen, K. A., and J. J. Champoux.** 1990. Plus-strand origin for human immunodeficiency virus type 1: implications for integration. J. Virol. **64:**6274–6277.
19. **Pullen, K. A., A. J. Rattray, and J. J. Champoux.** 1993. The sequence features important for plus strand priming by human immunodeficiency virus type 1 reverse transcriptase. J. Biol. Chem. **268:**6221–6227.
20. **Rausch, J. W., and S. F. J. Le Grice.** 2004. Binding, bending and bonding: polypurine tract-primed initiation of plus-strand DNA synthesis in human immunodeficiency virus. Int. J. Biochem. Cell Biol. **36:**1752–1766.
21. **Robson, N. D., and A. Telesnitsky.** 1999. Effects of 3′ untranslated region mutations on plus-strand priming during Moloney murine leukemia virus replication. J. Virol. **73:**948–957.
22. **Robson, N. D., and A. Telesnitsky.** 2000. Selection of optimal polypurine tract region sequences during Moloney murine leukemia virus replication. J. Virol. **74:**10293–10303.
23. **Sarafianos, S. G., K. Das, C. Tantillo, A. D. Clark, Jr., J. Ding, J. M. Whitcomb, P. L. Boyer, S. H. Hughes, and E. Arnold.** 2001. Crystal structure of HIV-1 reverse transcriptase in complex with a polypurine tract RNA: DNA. EMBO J. **20:**1449–1461.
24. **Schaefer-Klein, J., I. Givol, E. V. Barsov, J. M. Whitcomb, M. VanBrocklin, D. N. Foster, M. J. Federspiel, and S. H. Hughes.** 1998. The EV-O-derived

cell line DF-1 supports the efficient replication of avian leukosis-sarcoma viruses and vectors. Virology **248:**305–311.
25. **Sevilya, Z., S. Loya, A. Duvshani, N. Adir, and A. Hizi.** 2003. Mutagenesis of cysteine 280 of the reverse transcriptase of human immunodeficiency virus type-1: the effects on the ribonuclease H activity. J. Mol. Biol. **327:**19–30.
26. **Telesnitsky, A., and S. P. Goff.** 1997. Reverse transcriptase and the generation of retroviral DNA, p. 121–160. *In* J. M. Coffin, S. H. Hughes, and H. E. Varmus (ed.), Retroviruses. Cold Spring Harbor Laboratory Press, Cold Spring Harbor, N.Y.
27. **Telesnitsky, A., and S. P. Goff.** 1993. RNase H domain mutations affect the interaction between Moloney murine leukemia virus reverse transcriptase and its primer-template. Proc. Natl. Acad. Sci. USA **90:**1276–1280.
28. **Werner, S., and B. M. Whorl.** 2000. Asymmetric subunit organization of heterodimeric Rous sarcoma virus αβ: localization of the polymerase and RNase H active sites in the α subunit. J. Virol. **74:**3245–3252.
29. **Whitcomb, J. M., and S. H. Hughes.** 1992. Retroviral reverse transcription and integration: progress and problems. Annu. Rev. Cell Biol. **8:**275–306.
30. **Zhang, W.-H., E. S. Svarovskaia, R. Barr, and V. K. Pathak.** 2002. Y586F mutation in murine leukemia virus reverse transcriptase decreases fidelity of DNA synthesis in regions associated with adenine-thymine tracts. Proc. Natl. Acad. Sci. USA **99:**10090–10095.
31. **Zhang, X., and R. J. Crouch.** 1997. The isolated RNase H domain of murine leukemia virus reverse transcriptase. J. Biol. Chem. **272:**22023–22029.